APPLIED SCIENCES AND ENGINEERING

Electro-actuated valves and self-vented channels enable programmable flow control and monitoring in capillary-driven microfluidics

Yulieth Arango*[†], Yuksel Temiz*[‡], Onur Gökçe[§], Emmanuel Delamarche

Microfluidics are essential for many lab-on-a-chip applications, but it is still challenging to implement a portable and programmable device that can perform an assay protocol autonomously when used by a person with minimal training. Here, we present a versatile concept toward this goal by realizing programmable liquid circuits where liquids in capillary-driven microfluidic channels can be controlled and monitored from a smartphone to perform various advanced tasks of liquid manipulation. We achieve this by combining electro-actuated valves (e-gates) with passive capillary valves and self-vented channels. We demonstrate the concept by implementing a 5-mm-diameter microfluidic clock, a chip to control four liquids using 100 e-gates with electronic feedback, and designs to deliver and merge multiple liquids sequentially or in parallel in any order and combination. This concept is scalable, compatible with high-throughput manufacturing, and can be adopted in many microfluidics-based assays that would benefit from precise and easy handling of liquids.

INTRODUCTION

The use of microfluidics in lab-on-a-chip devices has already proven its benefits for a broad range of applications, including diagnostics, biochemistry, preclinical research, and cell biology, by reducing the time to results and the consumption of reagents while increasing the throughput of assays (*1–3*). Despite these strengths, most microfluidic implementations still rely on cumbersome methods to displace liquids, including complex components such as valves, actuators, pumps, and responsive materials (*4, 5*), and involve labor-intensive sample and chip preparation steps. These practical challenges contribute to limiting the scalability, portability, adoption, and commercialization of these devices, particularly if they are developed for point-of-care (POC) diagnostics applications (*6*). After the pioneering work from the Quake's group (*7*), monolithically integrated pneumatic valves have become a popular strategy for the scalable and programmable manipulation of liquids in microfluidic channels. However, such a manipulation has been typically addressed by developing complex microfluidic devices with moving structures and using bulky, specialized, and expensive peripherals, which also often require technically skilled users. A myriad of other integrated liquid control strategies, including manual (*8*), electrical (*9*), chemical (*10*), optical (*11*), magnetic (*12*), and thermal (*13*) actuation, have been developed, but they generally lack programmability and real-time feedback and still suffer from fabrication complexities and known issues associated with high-throughput manufacturing and integration of polydimethylsiloxane (PDMS) and hydrogels.

Digital microfluidics have emerged as an appealing alternative to program biochemical reactions precisely using droplets manipulated by means of various actuation principles without needing moving parts (*14*), such as electrowetting-on-dielectric (EWOD), dielectrophoresis, surface acoustic waves, and magnetic forces. Among these principles, EWOD has become the most extensively used technique,

yet it has several practical issues, such as the need for an immiscible oil phase to separate aqueous samples, high-voltage sources, hydrophobic coatings, transparent electrodes, and tens, if not hundreds, of external electrical contacts to address individual electrodes in high-density arrays (*15*). A continuous flow of samples, reagents, or particles passing through specific areas of a device is instead preferred or needed for most of applications covered by microfluidics (*16, 17*). For POC devices particularly, such a flow is generated using capillary action because it does not require peripheral equipment (*18*). This advantage is nevertheless hindered by limited flexibility in the flow control because the flow path and rate are defined by the design and materials and optimized for a specific assay. Following the work by the groups of Whitesides (*19*) and Yager (*20*), many research groups also spent substantial efforts to enhance the analytical performance of paper-based microfluidics by adding new functions to control the flow (*21*). We and other groups fabricated capillary-driven microfluidics with passive valves using precise structuring of hard materials, such as silicon, glass, and plastics (*22*). In general, it is challenging to implement precise, high-density, and programmable valves in paper microfluidics, and closed microfluidic channels implemented on other substrates suffer from complex fabrication, incompatibility with capillary-driven flow (e.g., hydrophobic polymers), and the difficulty of handling liquids (e.g., controlled merging or sequential delivery of liquids) without creating air bubbles.

Here, we present a new approach to control liquids in capillary-driven microfluidics by realizing programmable liquid circuits using a set of key functions (Fig. 1). Specifically with these circuits, (i) liquids can be stopped and routed where and when desired using a low-cost and portable peripheral device and a protocol applied from a smartphone, (ii) positions of the liquids can be monitored electronically, (iii) coflow or sequential flow of liquids can be generated, and (iv) synchronized and bubble-free merging of liquids can be done in closed and hydrophilic microchannels fabricated using high-throughput techniques. Stop-and-go flow control is based on e-gates (*23*), which use capillary pinning to stop flow based on Gibbs' inequality condition (*24*) and a low voltage (<5 V) electrowetting effect (*25*) to resume it. We extend this concept in programmable liquid circuits by providing a multiplexing capability and smartphone control and combining it
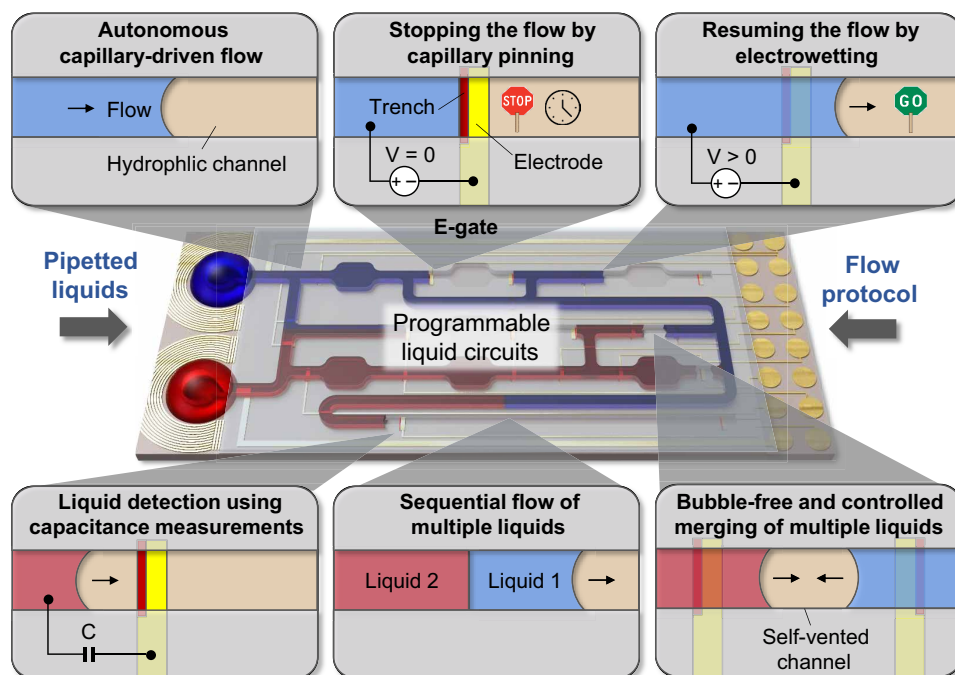
IBM Research–Zurich, 8803-Rüschlikon, Switzerland.
*These authors contributed equally to this work.
†Present address: ABB Research Centre, Segelhofstrasse 30-34, 5405 Baden, Switzerland.
‡Corresponding author. Email: yte@zurich.ibm.com
§Present address: Institute of Neuroinformatics, University of Zurich and ETH Zurich, 8057 Zurich, Switzerland.

Fig. 1. Programmable liquid circuits implemented in capillary-driven microfluidics. Concept on controlling, monitoring, sequential delivery, and merging of multiple liquids flowing in microfluidic chips using an array of electrically actuated microfluidic gates (e-gates) and a protocol applied from a smartphone. Liquids pipetted to a capillary-driven microfluidic chip autonomously flow inside microfluidic channels by capillary action until the flow is stopped by pinning the liquid meniscus at a trench-patterned orthogonal to the flow path. The flow is resumed by applying a potential difference (<5 V) between the liquid (positive) and an electrode patterned over the trench (ground). The location of the meniscus is monitored using capacitance measurements as a feedback. Using capillary valves with air vents and self-vented channels and e-gates, pipetted liquids can sequentially flow through the same channel in any order and combination, and liquids flowing in opposite directions can be merged without creating air bubbles.

with passive capillary valves and self-vented channels for controlled merging and sequential delivery of multiple liquids in a compact and portable system.

RESULTS

Operation principle of programmable liquid circuits

In their simplest possible implementation, the programmable liquid circuits use capillary forces to displace autonomously the liquids in microfluidic channels and capillary pinning sites at e-gates to stop and route liquids. Capillary pinning does not require external energy, and its magnitude is defined by the surface tension of the liquid, channel geometry, and contact angle of the liquid with the walls of the microchannels (26). This phenomenon has been used by other research groups in centrifugal microfluidics to create burst valves (27), in passive microfluidics for capillary trigger and stop valves (22), in microfluidic phaseguides for the controlled filling and emptying of microfluidic structures (28), and in microfluidic chips with virtual walls (29). In e-gates, the flow is resumed by applying a local potential difference between the meniscus and the pinning geometry through an integrated electrode, allowing the implementation of electrically controlled and independently addressable valve arrays in a compact chip layout. The design of programmable liquid circuits does not require specific rules, and the placement of e-gates and passive capillary valves can be done much like adding on/off switches or transistors to an electronic circuit. For example, e-gates can be placed to specific locations that are critical for an assay, e.g., after a mixing chamber to control a reaction time, along parallel microchannels for

selecting reagents, or in a regular array format for a more generic chip architecture. The layout and operation principle of an e-gate, an exemplary chip design, and the layouts of a passive microfluidic diode, a capillary stop valve, and a capillary trigger valve are given in fig. S1. In addition to the flow control elements, the microfluidic chip typically includes a loading pad, which can hold ~10 μl of liquid, microfluidic channels, and capillary pumps to draw a liquid using capillary forces, and a vent.

For the fabrication process, we prefer photolithographic patterning of silicon wafers because this process is compatible with high-volume manufacturing, supports capillary-driven flow without requiring post-fabrication treatments, and allows easy and precise integration of electrodes and dried reagents in sealed microchannels (30). We use moderately hydrophilic materials, such as epoxy-based SU-8 and dry-film resist (DFR) (~80° and ~70° advancing contact angles with water, respectively), for the side and top channel walls and pattern the e-gate trench with a sharp edge (~90° angle) on a more hydrophilic bottom layer, SiO_2, because this configuration gives a good balance for the wettability of the channel to both satisfy the Gibbs' inequality condition for pinning an liquid-air meniscus and generate a sufficiently high capillary pressure to displace the liquid elsewhere. Details of the chip fabrication involving three photolithography masks are provided in Materials and Methods and in fig. S2.

In our previous work, we showed the basics of an e-gate for stopping biological buffers, human serum, and artificial urine at a trench geometry with a semicircular shape (23). Here, we provide further analysis on the operation of e-gate arrays and their use in more complex microfluidic networks with different channel widths and

hydraulic resistances. An exemplary behavior of a meniscus at an e-gate is shown in fig. S3 and movie S1 for a 200-µm-wide, 15-µm-deep channel. The incoming meniscus first gets pinned at the center of the channel, follows the semicircular trench, and stabilizes within 200 ms by pivoting over the trench and following the contact angles of the other three walls. Upon application of a potential difference between the liquid (3 to 5 V) and the e-gate electrode (ground), the meniscus unpins from the center of the channel within 500 ms, in a way resembling to the release of a bowstring. E-gates implemented in narrower channels (50, 100, and 150 µm) showed a similar behavior (fig. S4); however, they could be activated at lower voltages and had a faster response time at the expense of lower stability (e.g., e-gates in 50-µm channels failed to hold the liquid for more than 1 min) caused by the reduced radius of curvature and the corresponding increased Laplace pressure exerted by the sidewalls. Wider channels (>500 µm), on the other hand, increased the risk of sagging of the DFR both during sealing the microfluidic chips and filling them with liquids. In addition, our experiments showed no correlation between the operation of e-gates and the upstream hydraulic resistance defining the flow rate of the liquid before reaching an e-gate, which ranged from 0.5 to 3 nl/s for the chips tested in this work. We also tested the stability of the capillary-driven flow and the operation of e-gates after long-term storage (16 months) of "ready-to-use" chips. Specifically, we observed that the functionality of these chips was retained when they were stored in the dark in an opaque wafer box (fig. S5). Here, we also show that the e-gates are compatible with whole blood (fig. S6A). However, they failed to pin the meniscus of lysed blood containing a high concentration of surfactant (fig. S6B). To achieve a stronger pinning for such a challenging sample, we replaced the hydrophilic DFR with a hydrophobic adhesive film (fig. S6, C and D).

### Programming the flow path using a smartphone

Unlike classical EWOD techniques developed to manipulate droplets (*31*) or continuous flows (*32*), e-gates do not use insulated electrodes or hydrophobic coatings since a reversible and large dynamic range modulation of surface wettability is not required. This implementation substantially simplifies the fabrication process and lowers the voltage needed to resume the flow of a pinned liquid (<5 V). This advantageous feature enabled us to implement a battery-powered peripheral device that interfaces with the microfluidic chip and is controlled via Bluetooth from a smartphone application (app). The device shown in Fig. 2A and detailed in fig. S7 uses a standard Arduino-based microcontroller, measures only $70 \times 12 \times 25$ mm³, can generate 0 to 5 V in 1.2 mV steps, and apply the generated potential difference to 2 of the 16 electrical contacts on the microfluidic chip in any combination. This brings another flexibility to the chip design because the polarity and the voltage level of each electrode can be programmed from the smartphone. We developed two apps to communicate with the device. One allows manual control over the parameters (e.g., amplitude and duration of the applied voltage and selected electrode pair) and the other works autonomously based on a programmable protocol that can be uploaded to the app. In a typical workflow, the Bluetooth communication between the phone and the device is established with just pressing a button on the app, a microfluidic chip with 16 electrical contacts is inserted to the device like inserting a universal serial bus (USB) memory to a computer, liquid samples with volumes ranging from 2 to 10 µl are pipetted to the chip, their flow conditions are controlled via the phone, and the chips are discarded after their use (movie S2).

In the following, we demonstrate the flexibility of programmable liquid circuits and the precise flow control achieved by using a smartphone. Figure 2A shows the app interface and the microscope images from a chip design with three parallel channels, each having four e-gates connected in series between areas mimicking a reaction chamber. Here, two chips with identical designs were used to generate two different flow sequences by manually activating the e-gates from the app (full sequence is provided in movie S3). We also used the same strategy to implement more complex microfluidic circuits comprising multiple options of flow paths, bypass channels, and microfluidic diodes (fig. S8). Counting on the reproducible and reliable operation of programmable liquid circuits, we leveraged the concept by designing a "microfluidic clock" that is only 5 mm in diameter, runs autonomously for about 1 hour without user intervention, and shows the time with 5-min intervals (Fig. 2B). Here, a 22-step protocol comprising 3-s e-gate activation duration at 3 V and 297 s waiting time for 11 e-gates was constructed as a table and uploaded to the app, which then executed the steps autonomously. The microfluidic chip and the peripheral device worked according to the protocol except for the last e-gate, which failed after holding the phosphate-buffered saline (PBS) solution for 50 min 30 s instead of 55 min (movie S4). This retention time is already long enough for many POC diagnostics applications but can be increased, if needed, using multiple e-gates connected using a cascade configuration, a wider channel for more stability, a less hydrophilic DFR, or a hydrophobic treatment applied to the Pd electrode (*23*).

Liquid control with feedback

In the experiments shown so far, we manually activated e-gates or applied a protocol while monitoring the position of the liquid using a microscope. However, in a potential end-user application, optical monitoring might not be available. In addition, multiple e-gates connected in different configurations, such as having several e-gates connected in parallel and others in series, might need different voltage levels or activation time. It is therefore ideal to monitor flow conditions continuously and have a feedback mechanism to synchronize the activation of e-gates with the actual location status of the liquids. On the basis of our previous work on flow monitoring using capacitance measurements (*33*), we were able to detect the arrival of the liquid to the e-gate and its activation by measuring the capacitance of the e-gate electrode without using additional components, fabrication steps, or external tools. The principle is based on measuring the change in the double-layer capacitance that is proportional to the area of the electrode in contact with the liquid. Measurement of the capacitance using the above-explained peripheral device required the addition of only two resistors and an analog switch. The peripheral device calculates the capacitance from the resistor-capacitor (RC) time constant after a 5-V pulse is applied to the selected electrode pair via a 10-megohm external resistor and when the voltage on the electrode pair reaches to 1 V. Then, the capacitance is discharged to 0 V via a 1-kilohm resistor for the next measurement. Keeping the maximum voltage of the electrode at 1 V minimizes the undesired electrochemical effects and the risk of activating the e-gate during the capacitance measurements. Because the activation of e-gates and measuring the capacitance would require applying different voltage levels to the same electrode pair, we decoupled their operation using an analog switch controlled by the microcontroller.

Figure 3A shows capacitance measurements during the sequential activation of three e-gates. When the liquid moves along the
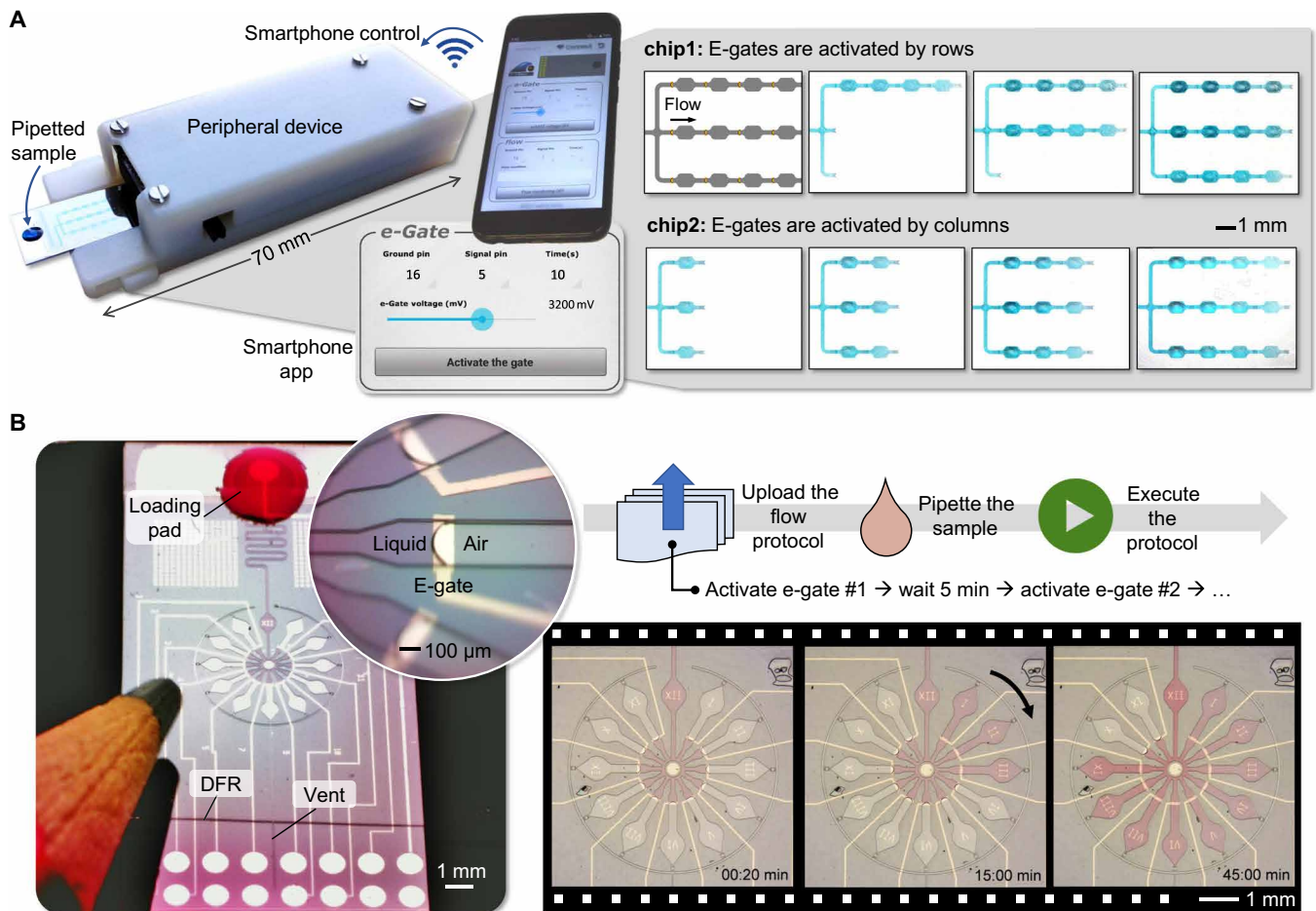
Fig. 2. Implementation of programmable liquid circuits using a portable peripheral device and a smartphone. (**A**) Capillary-driven microfluidic chips with identical designs were inserted to the peripheral, and 3 μl of PBS containing a blue dye was pipetted to the chips (left), e-gates were activated manually using a smartphone app (middle), and sequences of microscope images were captured during row-by-row (chip 1) and column-by-column (chip 2) activation of 12 e-gates (right). The first microscope image taken before pipetting the liquid (not shown) was subtracted from the others to highlight the position of the liquid in the flow path. (**B**) A "microfluidic clock" running autonomously based on a protocol applied from the phone. On the left is a photograph of the chip next to a pencil, after pipetting 3 μl of PBS solution with a red dye and before inserting the chip to the device. The liquid flowed through a 100-μm-wide and 15-mm-long channel and filled the center of the clock in 20 s (inset: tilted macro photograph of the pinned meniscus at a 200-μm-wide e-gate). On the right are microscope images of the chip, while e-gates were automatically activated by the smartphone every 5 min, representing the minutes of a 1-hour clock (see also movie S4). Photo credit: Yuksel Temiz, IBM Research–Zurich.

channel from the loading pad, the portable peripheral starts operating in the "flow monitoring" mode and records the measured capacitance with 1-Hz sampling rate. The capacitance increases 13 ± 3 pF on average upon pinning of the meniscus at the e-gate. Then, the system is switched to operate in the "electrogating" mode, resuming the flow by applying 5 V for 1 s, and immediately back to the flow monitoring mode. Because the electrode is partially wetted during the pinning and fully wetted after the activation (fig. S9A), resuming the flow results in another increase, 5 ± 3 pF on average, which can be used to detect the successful activation of an e-gate. If needed, the signal-to-noise ratio can be improved using larger electrodes or averaging at an expense of slower response time. The measured capacitance value is expected to change depending on the composition of the liquid, geometry of the electrode, and the distance between the electrodes. However, this variability should not be a concern for this work because we consider relative change in the measured value, not the absolute value, as an indicator for the wetting of the e-gates. For example, in Fig. 3B, we propose a simple algorithm that can be used to automati-

cally activate e-gates and adaptively tune the applied voltage and its duration based on the change in the measured capacitance. We also demonstrate that the capacitance measurements can be used to detect insertion of the chip to the peripheral device, pipetting the sample, and monitoring multiple e-gates (Fig. 3C). In theory, the method could be applied to measure from hundreds of e-gates at 1-Hz sampling rate using time-division multiplexing because the measurement typically takes less than 1 ms (e.g., 446 μs for 200 pF). A case with 15 e-gates is demonstrated in fig. S9B. Such a system, which fully traces all user actions and liquid positions over time, is very powerful and can remedy mistakes from users, operational failures, or deviations, and automatically generate a report for each device and test done. These functions can be particularly important for POC diagnostics applications.

Controlling multiple liquids using e-gate arrays
Many microfluidic applications require several liquids to flow in parallel with well-defined flow conditions, such as multiplexed (*34*)
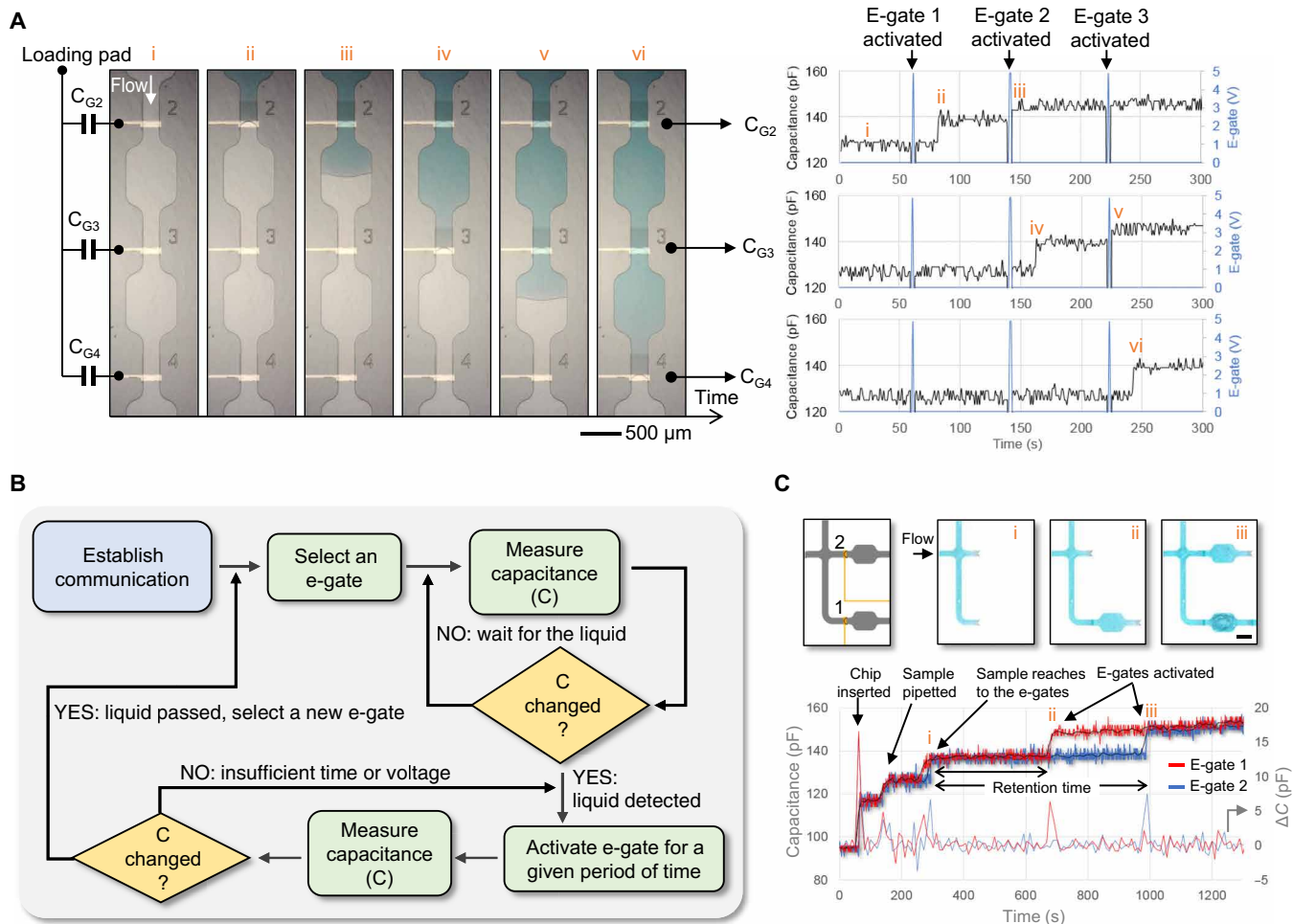
Fig. 3. An electrical feedback mechanism to detect the location of the liquid meniscus based on capacitance measurements from e-gate electrodes. (**A**) Microscope images showing three e-gates during their sequential activation (left). The capacitance of each e-gate (C_G), i.e., capacitance measured between the common electrode in the loading pad and the e-gate electrode, was measured continuously except during the activation of the e-gate (right). (i) The capacitances remained at 127 pF before the liquid reached the e-gates. (ii) C_{G2} increased to 140 pF after e-gate 1 was activated (not shown in the microscope images), and the sample reached to e-gate 2. (iii) E-gate 2 was then activated, and C_{G2} increased to 145 pF owing to increased surface area of the electrode in contact with the liquid. The capacitances of e-gate 3 (C_{G3}) and e-gate 4 (C_{G4}) showed a similar behavior when the sample reached to e-gate 3 (iv), after e-gate 3 was activated (v), and the liquid reached to e-gate 4 (vi). (**B**) Flowchart diagram of an algorithm that can be used to automatically activate e-gates based on a feedback from capacitance measurements. (**C**) The capacitance measured from two e-gates showing the change in the capacitance (ΔC) after the insertion of the chip, pipetting the sample, the menisci reaching to e-gates (i), and activation of e-gates (ii and iii). Microscope images on the top highlight the position of the menisci. Scale bar, 500 μm. Photo credit: Yuksel Temiz, IBM Research–Zurich.

or high-throughput (*35*) assays. Chip designs shown so far allow stop-and-go flow control of one liquid using a maximum of 15 e-gates, which is limited by the 16-contact pogo pin connector. The peripheral electronics can easily be scaled to address more e-gates, but this would increase the area of the chip for accommodating more external electrical contacts. Instead, we sought to increase the number of e-gates by connecting several of them to the same contact (ground electrode) and increase the number of liquids by adding liquid selection electrodes (positive electrode) to their respective loading pads (Fig. 4A). Here, e-gates for all liquids are connected to each other for a given location. The flow of a liquid at that location is triggered by applying a potential difference between the liquid selection electrode and the common e-gate electrode, much like a row/column selection in a matrix. This concept was illustrated using a microfluidic chip (1×2 cm^2) with four loading pads, microchannels in a race track–like configuration, and a total of 100 e-gates (Fig. 4B). Each channel

had 25 e-gates connected to 12 external electrical contacts. Colored PBS solutions were pipetted on the corresponding loading pads (~1.5 μl per pad) as shown in the upper part of Fig. 4B. Liquids could be individually controlled by selecting the corresponding electrode pair from the smartphone app. For the activation of the second e-gate connected to the same contact, the flow of the liquid could be resumed by applying the same voltage level (5 V), but the activation delay was slightly longer. We tested this delay using a design having 10 e-gates connected in parallel (fig. S10). The activation delay gradually increased from 0.5 to 10 s for the 10th e-gate, probably because of the voltage drop on the previously activated e-gates and the increased capacitance, resulting in a higher RC time constant. The increase in the measured capacitance when a liquid passes an e-gate and moves to the next one in a channel (Fig. 4C) can be used both to track the position of individual liquids and mitigate activation delays. Furthermore, these delays are unlikely to be problematic for many applications
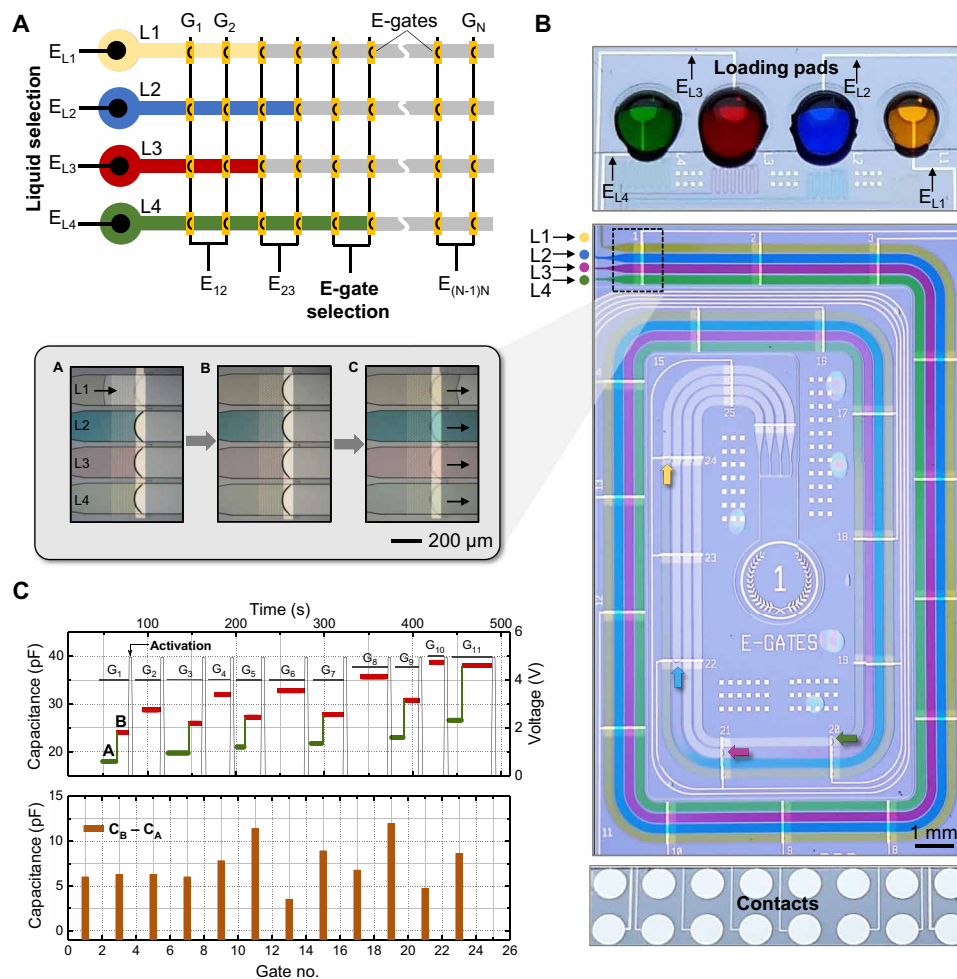
Fig. 4. Efficient control of multiple liquids using e-gates connected in parallel. (**A**) Multiple liquids are controlled independently by applying a potential difference between the liquid selection electrode (E_L), which is patterned in the loading pad, and the e-gate selection electrode (E_N), which is common for all liquids for a given position and connected to the ground. Multiple e-gates can be electrically connected to the same external contacts, such as two consecutive e-gates connected to the same electrode as shown in the illustration. (**B**) Photograph of a tested chip containing four independent channels in a race-like configuration and 25 e-gates per channel, which are connected to 12 contacts. The upper part shows the configuration of the four loading pads providing the dyed PBS solutions to the corresponding channels and the routing of liquid selection electrodes (E_L) patterned on the loading pads. Inset shows the magnified image of the dyed samples controlled by a set of e-gates and focused on the yellow solution: before arriving to the e-gate (frame A), stopping at the e-gate (frame B), and passing over it after activation (frame C). (**C**) The upper plot shows capacitance measurement between the electrode at the indicated e-gate and the electrode at the loading pad for one of the solutions before it arrives to the e-gate [green, frame A in inset of (B)] and when it stops [red, frame B in inset of (B)]. The continuous vertical black line indicates the voltage (5 V) applied to activate the e-gate. The lower plot shows the difference in the capacitance values when measured before and once the meniscus arrives to the e-gate. Photo credit: Yulieth Arango, IBM Research–Zurich.

where biochemical processes or experiments involving cells often occur over tens of minutes.

Programming sequential flow of multiple liquids

Implementing assays, such as enzyme-linked immunosorbent assay (ELISA), in microfluidic systems requires a seamless sequential flow of liquids having various reagents and analytes. Specifically, no air bubbles or uncontrolled liquid interfaces should occur between two liquids flowing consecutively in a same flow path. This type of sophisticated manipulation and routing of multiple liquids has been extensively studied using active pumping and/or mechanical valves at the expense of manufacturability, portability, and user friendliness and still is a long-lasting challenge for passive microfluidic systems being developed for POC diagnostics. A prominent example of com-

plex flow control in capillary-driven microfluidics is the concept of "capillarics" introduced by Safavieh and Juncker (*36*). Although sequential flow of pipetted reagents and flow reversal were demonstrated using capillary valves, the flow conditions were preprogrammed in the design and fabrication of the chips, the timing required precise adjustment of the volumes of the pipetted liquids, and the implementation had limitations associated to the use of PDMS in capillary-driven microfluidics. E-gates, in contrast, use materials inherently compatible with capillary-driven flow, and flow conditions can be programmed after fabrication. Nevertheless, e-gates alone do not enable liquid merging and sequential flow. This can be solved by combining e-gates with capillary valves and using local electrolysis of water at specific e-gates to segment liquids. A notable example is provided in Fig. 5, where a sequence of input liquids can be selected to
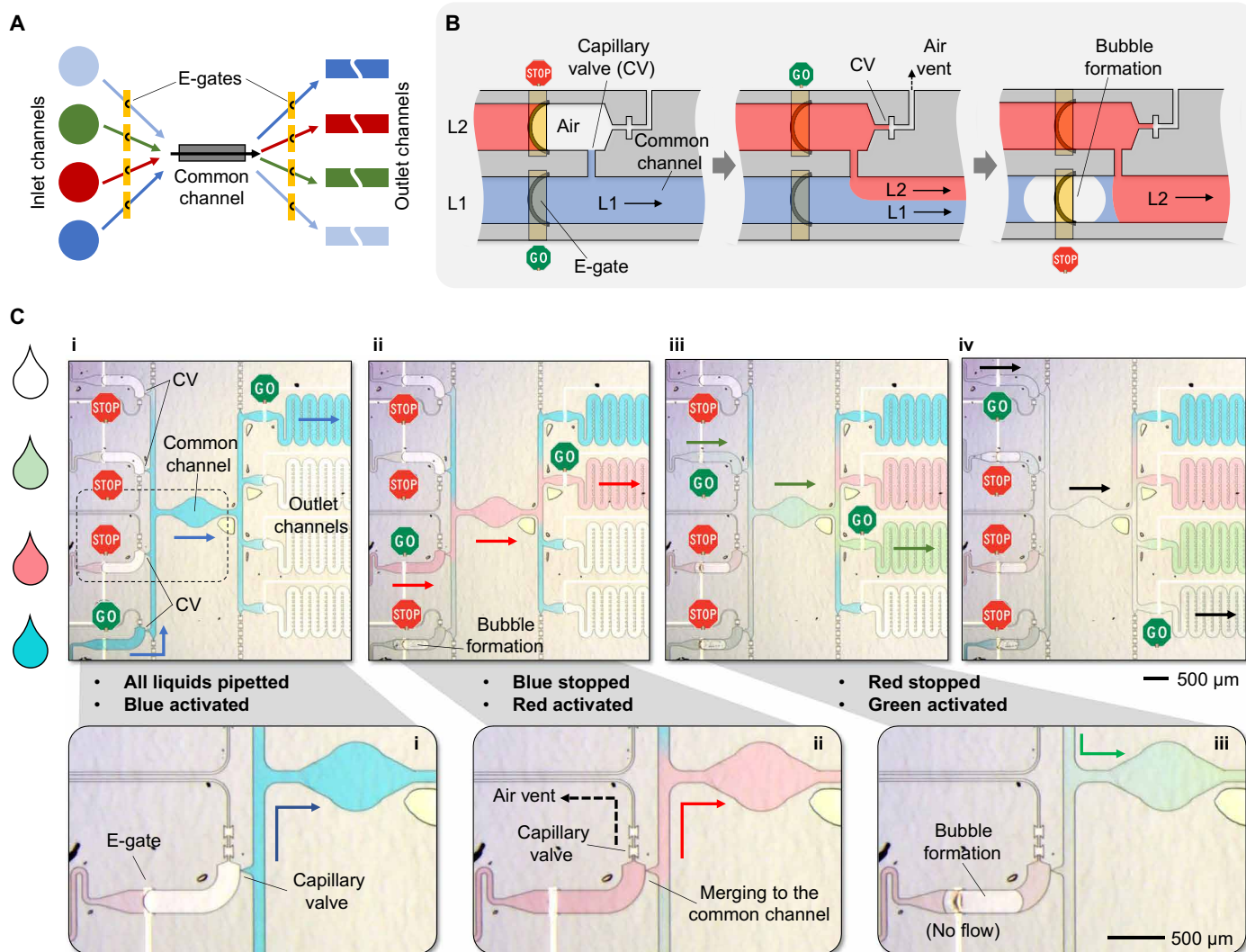
Fig. 5. Advanced liquid circuits and sequential delivery of liquids implemented using e-gates and capillary valves with air vents. (A) Concept showing multiple liquids controlled by e-gates and flowing through a common channel in any combination and any sequence. **(B)** A capillary valve with an air vent enables merging of multiple liquids without creating an air bubble while the flows of liquids are controlled by e-gates. In this illustration involving two liquids, liquid 1 (L1) flows in a channel and has a connection to a second channel via a capillary valve (left). The flow of liquid 2 (L2) is resumed by activating its e-gate (middle). It then merges to L1 at the capillary valve by pushing the air out through the air vent, which has another valve preventing L2 entering the vent. Both liquids flow through the common channel until the flow of L1 is blocked by a bubble, which is formed through hydrolysis by applying a sufficiently high potential difference to the e-gate (right). **(C)** Experimental results showing sequential flow of liquids through a common channel. (i) PBS solutions in four colors (transparent, red, green, and blue) were pipetted to their respective loading pads and retained by e-gates. First, the flow of PBS in blue was initiated, filling the common channel and stopping at the valves connecting to other channels. Additional e-gates located after the common channel were used to direct the liquid to one of the four outlet channels. (ii) The flow of PBS in blue was completely blocked by a bubble created by applying +15 V DC between the e-gate electrode (positive) and the common electrode in the loading pad (ground). Then, the flow of PBS in red was initiated by activating its e-gate, merging it to the common channel through the capillary valve holding the PBS in blue. (iii and iv) Similarly, the remaining two liquids (green and transparent) flowed sequentially through the common channel after the flow of the previous liquid was blocked and corresponding e-gates were activated. Arrows matching to the color of the liquid highlight the flow direction, and the whole sequence can be seen in movie S5. Photo credit: Yuksel Temiz, IBM Research–Zurich.

pass through a common flow path and sorted to specific outlet channels (Fig. 5A). This concept is based on two key features: (i) controlled merging of a liquid to a channel that is already filled with another liquid using a capillary valve having an air vent, and (ii) blocking the flow of a liquid by electrochemically generating a bubble using an e-gate electrode (Fig. 5B).

We demonstrate controlled merging and sequential delivery of liquids using a test chip having four loading pads, a common chan-

nel, four outlet channels, and two e-gates per liquid located before and after the common channel (fig. S11, A and B). Figure 5C and movie S5 show the experimental result where 2 μl of colored PBS solutions were pipetted to the chip and hold in place by their respective e-gates. In contrast to classical capillary-driven microfluidic systems where multiple liquids should be introduced one after the other depending on the desired protocol, here, all liquids can be pipetted at the same time, giving full control to the smartphone protocol to

achieve a more flexible, synchronized, and error-free operation. Following the activation of two specific e-gates, the first liquid (blue in this case) started to fill the common channel and a target outlet channel but remained pinned by the capillary valves elsewhere. This design is symmetric, and any liquid can be selected to pass first. The flow of the first liquid was then stopped by creating a bubble by applying a 15-V potential difference between the liquid (ground) and the e-gate electrode (positive) for a few seconds. The flow of the second liquid (red) was initiated by merging it to the common channel through the capillary valve with the air vent, where the first liquid had already been pinned. The same process was repeated for the remaining liquids. This concept can also be used to create controlled coflows of multiple liquids in any combination by merging new liquids to a channel already filled with a liquid (movie S6 and fig. S11C).

Self-venting mechanism in microfluidic channels

Flow inside microchannels requires displacing air unless channels are left open (37) or made from permeable materials (38). Some microfluidic devices may require air vents with reduced dimensions or very long paths extended from the channel outlet to the air vent (e.g., the chip in Fig. 4B). Routing of multiple air vents to the edges of the chip may become a serious design challenge for more complex microfluidic circuits involving multiple liquids and capillary stop valves with vents. As an example, air vents of the chip shown in Fig. 5C had to be routed back to the side of the loading pads. In some cases, improper placement of air vents might lead to failures (e.g., liquid blocking the vent) or, even worse, biosafety issues with a body

fluid sample potentially leaking outside the chip. Sometimes, vertical openings are created through sealing layers and packages, but this is cumbersome in terms of fabrication. Programmable liquid circuits offer great control and flexibility for manipulating liquids but cannot merge them arbitrarily without a new venting strategy. To this end, we introduce the concept of "self-vented channels" and propose a fabrication process compatible with e-gates, which is detailed in Materials and Methods.

The concept is based on partial wetting of the cross section of the flow path, similarly to liquid microchannels formed using a wettability contrast (39) or virtual electrowetting channels (32). We achieved this easily by creating side stripes of black silicon in the bottom layer of a closed microfluidic channel. Figure S12A illustrates the operation principle and experimental results of the self-venting mechanism, and movie S7 shows two menisci of PBS flowing in opposite directions and merging without trapping an air bubble. Self-vented channels can be combined with the creation of trenches comprising black silicon for pinning liquid at e-gates using a common deep reactive-ion etching (DRIE) step (Fig. 6A). The electrical insulation of the liquid from the black silicon and silicon wafer substrate is achieved by depositing a conformal, thin layer of Al_2O_3 (fig. S12B). This insulation is important to ensure multiplexing capabilities by being able to activate selected e-gates without cross-talk with other e-gates through the silicon substrate. The resulting e-gates are fully functional (activation ~1 s with 4-V activation; Fig. 6B). Figure 6C shows an exemplary design where trenches for e-gates and pinning structures for self-venting are patterned in black silicon, the surface of the wafer is passivated using
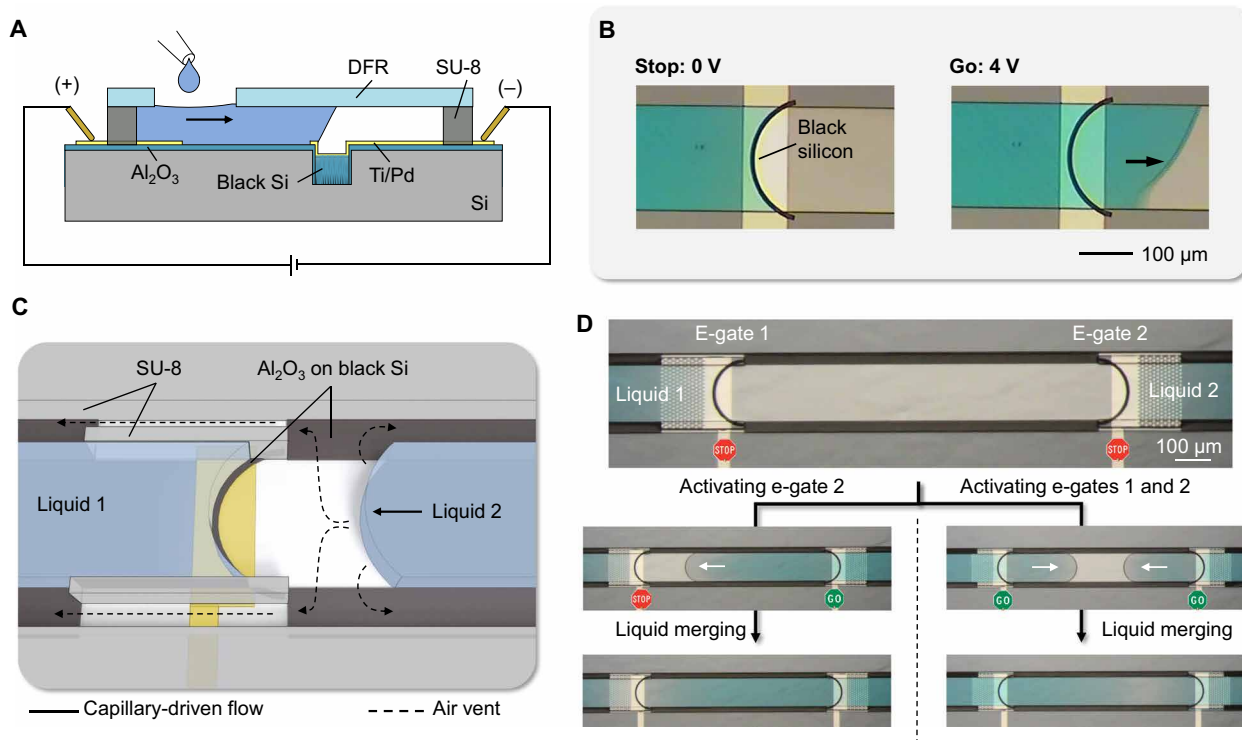
Fig. 6. Self-vented channels and e-gates. (**A**) Side view of the components for electrogating using a black silicon area instead of a trench for the implementation of e-gates. (**B**) Microscope images showing the stop-and-go control of the liquid flow. (**C**) Three-dimensional (3D)–rendered illustration showing liquid 1 pinned at the e-gate and liquid 2 merging to liquid 1 without creating an air bubble owing to side air vents patterned in black silicon. (**D**) Examples of merging two liquids stopped at the e-gates (upper frame): Microscope images on the left show bubble-free merging after e-gate for liquid 2 was activated, and the ones on the right show a case where both e-gates were activated at the same time using a common electrode (from movie S8). Photo credit: Yulieth Arango, IBM Research–Zurich.

Al_2O_3, and electrodes and microfluidic channels are patterned as previously explained. Figure 6D and movie S8 show the experimental results from this configuration where two liquid menisci are merged in different combinations using the smartphone app.

DISCUSSION

The concept of programmable liquid circuits presented here (i) enables the implementation of generic, programmable, and portable microfluidic systems that can be fabricated using high-throughput techniques; (ii) is simple to use; (iii) allows fast and reliable control of multiple liquids; and (iv) provides real-time feedback on the flow conditions of liquids. This concept combines e-gates with passive microfluidic valves and self-vented channels and has many advantages compared with other liquid-handling techniques. First, compared with microfluidic systems with actively pumped liquids, programmable liquid circuits do not require any labor-intensive preparation, such as preparing syringes and manually connecting tubings to microfluidic chips, and they can work with a small droplet of sample or reagent. Capillary forces are used to drive liquids without using any peripheral equipment to create a pressure gradient. The flow is stopped passively by capillary pinning at a trench; therefore, no external energy is required while holding the liquid in place, which can leave the necessary time for functions often implemented in microfluidics such as dissolving reagents, reactions, separating analytes, stimulating cells, etc. Activation of the flow is achieved by applying 3 to 5 V to a selected e-gate for less than 1 s. This allowed us to control many e-gates using a battery-operated device, which is about the size of a matchbox and communicates with a smartphone via Bluetooth. We also showed that the operation of chips is not compromised after 16 months of storage. Second, each e-gate can be individually monitored in real time using capacitance measurements as a feedback to the user (e.g., warning about a failure). In addition, such a feedback can be used in an algorithm to optimize the e-gate parameters and to run an assay protocol fully autonomously. Third, multiple e-gates can be connected to the same external electrical contacts to control continuous flows of multiple liquids in several locations, which is something that cannot be easily implemented in digital microfluidics using EWOD.

Like many other techniques, programmable liquid circuits have limitations. First, the pinning capability of e-gates is challenged when solutions with surfactants, human serum, or whole blood are used. A stronger capillary pinning can be achieved by changing the geometry of the channel (e.g., wider channels), making the electrodes hydrophobic (23), or using a less hydrophilic film for the top sealing layer (fig. S6). Second, unlike mechanical valves, an e-gate can be activated and deactivated only once unless the bubble formed to stop the flow is removed electrochemically. If the flow of a liquid needs to be stopped and resumed repeatedly, an array of e-gates can be patterned along the flow path, preferably in the capillary pump. In addition, the chips are not meant to be reusable not only because it would not be practical to dry channels, which are filled with liquids, but also reusing the chips is not desirable for POC applications where cross-contamination between patients' samples can be an issue. Third, although activating a single e-gate takes less than 1 s, connecting more e-gates to the same electrode results in an additional delay in the activation time (e.g., 10 s for 10 e-gates). If a fast response is critical for the application, this delay could be reduced by having the electrode biasing the liquid closer to each e-gate instead of having it only in the loading pad. This would also help improve the precision of the capacitance measurements for the feedback by reducing the distance and thus resistance between two electrodes. Fourth, we fabricate these circuits using silicon wafers and clean room processes, which are often considered "expensive" and not easily accessible by the research community working on microfluidics. This statement is generally true for high-end complementary metal-oxide semiconductor (CMOS) chips (e.g., microprocessors) or low-volume prototyping. However, there are many examples of microfluidic implementations benefiting from the unique properties of silicon and the well-established manufacturing infrastructure developed for processing it (40), a prominent and commercially successful one being the i-STAT POC device from Abbott. In addition, our process is simple and efficient: It requires only three photolithography masks, enables the fabrication and sealing of hundreds of chips simultaneously, and takes the advantage of precision to fit many e-gates in a small footprint, all potentially contributing to reduction in cost. The process is also CMOS compatible; therefore, high-density arrays of e-gates can be postfabricated on top of electronic chips and can be individually addressed using row/column selection. Moreover, we think that the concepts demonstrated here can be implemented in other materials, such as glass or hydrophilic polymers, as long as the manufacturing process enables the patterning of a capillary pinning structure and integrated electrodes.

Programmable liquid circuits open exciting possibilities for lab-on-a-chip applications: Microfluidic devices can have generic architectures that can be controlled on demand using a smartphone or be fully automated with a protocol easily changed. For example, holding a liquid for tens of minutes can be used to study cells or reaction kinetics in immunoassays and molecular assays. Programming the delivery of samples, reagents, and rinsing buffers flowing sequentially or in parallel through the same channel can eliminate the need for manual actuation or sliding mechanisms [e.g., V-chip technology (41)], cartridges loaded with reagents, and sophisticated lab-on-a-disk designs. Programmable liquid circuits can also be combined with our recent invention, self-coalescence modules (42), to realize sample-in-answer-out lab-on-a-chip devices having programmable and precise spatiotemporal control on the dissolution of integrated reagents. One particularly interesting application can be multiplexed homogenous phase assays, such as assays measuring multiple enzymatic reactions. It is typically challenging to synchronize the flow of the reagents and to measure the reaction kinetics of multiple analytes using a single reader. Here, programmable liquid circuits can ensure that all reagents arrive in desired areas in a timely manner, and specific enzymatic reactions can be quenched when desired for the acquisition of a stable, end-point signal using a reader. In addition, the concept can be used to pattern biomolecules on surfaces using cross flows without needing manual manipulation of channels as in the case of highly multiplexed micromosaic immunoassays (43). Self-vented channels may be used to address one of the main failure mechanisms in microfluidics, which is the formation of bubbles during the filling of microchannels, merging multiple liquids, or locally as a consequence of the assay protocol (e.g., electrochemistry, thermocycling in PCR, gaseous by-products). This concept also opens intriguing possibilities involving programming counterflows of different liquids. Liquids can be brought into contact with well-defined position, and starting time and reactions at the interface between liquids can be precisely studied or implemented, such as crystallization processes, diffusion processes, or kinetics (enzymatic reactions).

In conclusion, the versatility, simplicity, and scalability of this concept provide a compelling technology for the development of portable, smart, and interactive lab-on-a-chip devices that can manipulate multiple liquids autonomously with minimal human intervention.

MATERIALS AND METHODS

Chip design and photolithography
Layouts of the microfluidic chips were designed using L-Edit software (Mentor Graphics) and converted to GDSII file format. A DWL-2000 (Heidelberg Instruments) laser lithography system was used to transfer layouts to glass/Cr photomasks (NanoFilm, USA). The chips were fabricated on 4-inch Si wafers (single side polished, 525 ± 25–μm thickness, N/Phos doping, 1 to 10 ohm·cm resistivity, <100> orientation) purchased from Si-Mat (Germany). A mask aligner (MA6, SÜSS MicroTec AG, Germany) with i-line UV light power density ($13 \ mW/cm^2$) was used to expose photoresists. A 3.3-μm-thick AZ 4533 (MicroChemicals GmbH) positive-tone photoresist was used as a mask for the etching of the SiO_2 layer and the patterning of metal electrodes using the lift-off process. The photoresist was spin coated at 4000 rpm for 40 s, baked at 110°C for 1 min, exposed to UV light (dose, $91 \ mJ/cm^2$), and developed in AZ 400K developer. Microfluidic channels were fabricated by patterning a 15-μm-thick SU-8 (SU-8 3010, MicroChem Corp.) using an optimized recipe to achieve <5-μm minimum feature size and spacing. The recipe consisted of spin coating (40 s at 1500 rpm), baking (2 min 65°C + 5 min 95°C), exposure ($85 \ mJ/cm^2$), postexposure baking (1 min 65°C + 2 min 95°C), development [90 s using propylene glycol methyl ether acetate (PGMEA)], and, finally, hard baking (150°C, 5 min).

Fabrication of e-gates with semicircular trenches
The fabrication process of chips shown in Figs. 2 to 5 involved three photolithography steps for (i) etching semicircular trenches in SiO_2, (ii) patterning electrodes using metal lift-off process, and (iii) patterning microfluidic channels in SU-8 (fig. S2). First, an Si wafer with a 3-μm-thick thermally grown SiO_2 was cleaned with an O_2 plasma (600 W, 600 sccm, 5 min) and treated with hexamethyldisilazane vapor at 110°C. Following the patterning of AZ 4533 using the photomask for trenches, SiO_2 was anisotropically etched to a depth of 1.9 μm in an inductively coupled plasma etching tool (PlasmaPro 100, Oxford Instruments) at an etch rate of 250 nm/min. After removing the photoresist mask in the O_2 plasma asher and treating the wafer with HMDS, a new layer of AZ 4533 was patterned for the metal lift-off process. A 5-nm-thick Ti (adhesion layer) and a 80-nm-thick Pd (electrode layer) were deposited using e-beam evaporation (Evatec BAK 501), while the wafer was tilted approximately 40° and rotated at 20 rpm to ensure conformal coating of the metal layer over the trenches etched in SiO_2. The wafer was then immersed into acetone for 10 min to reveal the electrodes (lift-off). A mild and short (5 to 10 s) ultrasonic agitation was applied every minute to break the continuous metal layer and accelerate the lift-off process. The wafer was rinsed in isopropyl alcohol (IPA) and dried using a flow of N_2. Following a 2-min O_2 plasma treatment (200 W, 200 sccm) and 2-min dehydration at 150°C, 15-μm-thick SU-8 was patterned for the microfluidic structures. The wafer surface was protected using AZ 4533 before dicing the wafer to half of its thickness. The wafer was then cleaned in acetone and IPA to remove the photoresist protection as well as the residues from the dicing process. Rectangular strips of a 50-μm-thick DFR [DF-1050 from Engineered Materials Systems (EMS) Inc., USA] were aligned and laminated over the microfluidic structures at 45°C. Last, "ready-to-use" chips were singulated by manually cleaving the wafer from the dicing cuts. The DFR was not exposed to UV nor to temperature after its lamination. For the long-term storage experiments (fig. S5), laminated chips were kept in an opaque wafer box and tested after 16 months. For the electrogating of the lysed blood (fig. S6, C and D), we replaced the DFR with a hydrophobic adhesive film (ARseal 90880, Adhesives Research Inc.) to achieve a stronger capillary pinning at e-gates.

Fabrication of self-vented microfluidic channels
Microfluidic chips designed to demonstrate the self-venting mechanism (fig. S12A) were fabricated on an Si wafer with a 200-nm SiO_2 layer. First, the patterns to be converted to black silicon were wet etched into the SiO_2 layer by immersing the wafer in a (1:10) buffered hydrofluoric acid (BHF) solution for 3 min. Then, "physical channels" were structured in SU-8. The wafer was partially diced to half of its thickness and cleaned in acetone and then IPA. Black silicon was formed by etching Si regions using DRIE (Alcatel AMS 200). SiO_2 and SU-8 layers acted as hard masks for this process. DRIE was done after the partial dicing to protect fragile needle-like black silicon structures (surrounded with hydrophobic C_4F_8 polymeric passivation) from the dicing process. Because the wafer was still in one piece after partial dicing, DRIE and DFR lamination steps could be done at a wafer level without using a support substrate or wafer. Last, sealed chips were singulated by cleaving the wafer and used without requiring a further postfabrication treatment.

Integration of e-gates to self-vented channels
For the microfluidic chips combining electrogating and self-venting (Fig. 6), the pinning geometry of e-gates was implemented by creating a semicircular pattern of black silicon instead of an etched trench. The fabrication process (fig. S12B) started with an Si wafer without an SiO_2 layer and followed by (i) creating black silicon regions in DRIE, (ii) removing of the photoresist mask and residues of C_4F_8 polymeric layer using O_2 plasma ashing, (iii) deposition of 15-nm Al_2O_3 passivation on the entire wafer using atomic layer deposition (FlexAL, Oxford Instruments; deposition rate, 0.12 nm per cycle), (iv) patterning metal electrodes, and (v) patterning microfluidic structures in SU-8. The wafer was then protected with a photoresist, diced partially, cleaned, sealed, and singulated as explained previously. Here, the dicing and the following cleaning process did not adversely affect the mechanical stability of the black silicon layer, which was covered with Al_2O_3 and photoresist protection.

Smartphone applications
Android applications were written in Java using the DroidScript (http://droidscript.org) platform. The first application allows manual control on the parameters for the selected electrode pair and the applied voltage and its duration, while the second application autonomously executes a protocol comprising a list of electrogating and flow monitoring steps. In both applications, after the Bluetooth connection is established between the application and the peripheral device, and when a button is pressed to activate or deactivate electrogating or flow monitoring, the application concatenates all parameters in a single string and sends to the peripheral device in JavaScript Object Notation (JSON) format. For example, to apply 3.5-V potential difference between contacts #1 and #16 for electrogating, the string {"PositivePin":"1","GroundPin":"16","Electro-gating":"1", "FlowMonitoring":"0", "Voltage":"3500"} is sent to the peripheral device.

JSON file format was preferred to easily add or remove parameters for alternative or future versions of the platform, which can potentially fetch the parameters from the Cloud. For the application, which automatically executes a protocol, the data were parsed from a CSV (comma-separated values) file, indexed, and sent to the peripheral device according to the timing information defined for each step.

Design and implementation of the peripheral device
The circuit diagram and the operation principle of the portable peripheral can be found in fig. S7. The key components of the device are a 1.27-mm-pitch, 16-contact Pogo pin connector (855-22-016, Mill-Max) to enable an easy and reliable electrical connection to microfluidic chip, an Arduino microcontroller (Pro Micro 5 V/16 MHz, SparkFun Electronics), a Bluetooth module (RN-42, Microchip Technology) connected to the microcontroller via an universal asynchronous receiver-transmitter (UART) bus, a 12-bit digital-to-analog converter (DAC) (MCP4725, Microchip Technology) to generate the e-gate voltage, and two 16-channel analog multiplexers (74HC4067, Nexperia) to select an electrode pair in any combination. A 3.7-V, 110-mAh rechargeable lithium-polymer battery powers the device, and an MCP73831 charge management controller chip (Microchip Technology) charges the battery via the USB port of the Arduino microcontroller. A step-up converter, XC9142 (Torex), was used to convert 3.7 V to 5 V, which is required for the microcontroller, DAC, and multiplexers. The Bluetooth module, which runs at 3.3 V, was powered via a linear voltage regulator (MCP1700, Microchip Technology) and connected to the microcontroller (5 V) through TXB0102 (Texas Instruments) bidirectional voltage-level translator. Because it is not possible to perform electrogating and flow monitoring simultaneously on the same electrode pair due to different voltage levels involved, an analog switch (TS5A3166, Texas Instruments) controlled via the microcontroller was used to connect the positive electrode of the microfluidic chip either to the DAC or to the flow monitoring circuit. Flow monitoring is based on measuring the double-layer capacitance of the electrode pair by applying a 5-V voltage pulse through a known resistor (1 megohm) and measuring the charging time, thus RC time constant, when the voltage across the electrode pair reaches to 1 V. Then, the capacitance was immediately discharged to 0 V through a smaller resistor (1 kilohm). Because the maximum potential difference of the electrode pair was limited to 1 V, electrochemical corrosion of the electrode during long flow monitoring experiments was minimized (e.g., 20-min-long measurement in fig. S9). All components were assembled inside a housing with a spring-loaded locking mechanism, which was designed in FreeCAD software and printed using a Stratasys Dimension Elite three-dimensional (3D) printer. Last, an RGB LED (SK6812) was placed inside the housing to show the status of the device by diffusing light through the translucent housing.

Arduino microcontroller code
The code for the Arduino microcontroller was written using the Arduino Software (www.arduino.cc/en/Main/Software). Five libraries were used: (i) Wire.h to enable I2C communication, (ii) CD74HC4067.h for controlling the multiplexers, (iii) Adafruit_MCP4725.h to communicate with the DAC, (iv) ArduinoJson.h to transmit data between the app and the peripheral in JSON format, and (v) Adafruit_NeoPixel.h to control the RGB status LED. The code uses a simple execution flow. After the initialization of the variables and the libraries, the code waits until the Bluetooth communication is established. The incoming string in JSON format from the phone is parsed to separate variables that register posi-

tive and ground contacts of the microfluidic chip, e-gate voltage, and the operation mode (electrogating, flow monitoring, or idle). Then, the code sets the multiplexers, the DAC, and the analog switch. For example, electrogating function is executed by setting the DAC voltage to the given value and connecting the DAC output to the microfluidic chip via the analog switch. The code loops every 100 ms to check whether there is a new incoming data from the phone and executes the selected function until it receives a string with {"Electrogating":"0, "FlowMonitoring":"0"} (i.e., idle mode). To record the data for plots, all parameters and the measured capacitance values were sent back to the phone (Bluetooth) or the computer (USB) every second.

Liquid samples
All chemicals were purchased from Sigma-Aldrich unless otherwise specified. Colored solutions of PBS were prepared by dissolving erioglaucine disodium (blue), amaranth (red), and tartrazine (yellow) at a concentration of 1 mg/ml. Green color was obtained by mixing the solutions in blue and yellow. Test blood samples used in fig. S6 were purchased from Transfusion Interregionale CRS, Switzerland, which provides samples for research by collecting them from anonymous donors using a 9-ml tube coated with EDTA as an anticoagulant (article number 92000). For lysing red blood cells (fig. S6, B to D), a solution of 10 mM Triton X-100 surfactant was prepared in PBS. A 50-μl solution was pipetted in a 200-μl reaction tube. The lid was let open to allow the solvent to dry completely. Whole blood (50 μl) was added to the reaction tube with dried reagents, vortexed for 5 s, and incubated for 5 to 10 min to achieve complete lysis of red blood cells.

Experimental setup and image processing
Images and videos of microfluidic chips were recorded using a Nikon 1 J3 camera connected to a Leica MZ16 stereomicroscope. Time-lapse microscope images in Figs. 2A and 3C and fig. S8B were postprocessed using the ImageJ software to enhance the contrast and highlight the position of the liquid. The best contrast was achieved by color-inverting all RGB images, subtracting the first image, which was taken before pipetting the sample, from the consecutive images and reinverting resultant images.

SUPPLEMENTARY MATERIALS
Supplementary material for this article is available at http://advances.sciencemag.org/cgi/content/full/6/16/eaay8305/DC1

REFERENCES AND NOTES
1. P. Yager, T. Edwards, E. Fu, K. Helton, K. Nelson, M. R. Tam, B. H. Weigl, Microfluidic diagnostic technologies for global public health. *Nature* **442**, 412–418 (2006).
2. E. K. Sackmann, A. L. Fulton, D. J. Beebe, The present and future role of microfluidics in biomedical research. *Nature* **507**, 181–189 (2014).
3. L. Y. Yeo, H.-C. Chang, P. P. Y. Chan, J. R. Friend, Microfluidic devices for bioapplications. *Small* **7**, 12–48 (2011).
4. A. K. Au, H. Lai, B. R. Utela, A. Folch, Microvalves and micropumps for BioMEMS. *Micromachines* **2**, 179–220 (2011).
5. W. Hilber, Stimulus-active polymer actuators for next-generation microfluidic devices. *Appl. Phys. A.* **122**, 751 (2016).
6. C. D. Chin, V. Linder, S. K. Sia, Commercialization of microfluidic point-of-care diagnostic devices. *Lab Chip* **12**, 2118–2134 (2012).
7. M. A. Unger, H. P. Chou, T. Thorsen, A. Scherer, S. R. Quake, Monolithic microfabricated valves and pumps by multilayer soft lithography. *Science* **288**, 113–116 (2000).
8. D. B. Weibel, M. Kruithof, S. Potenta, S. K. Sia, A. A. Lee, G. M. Whitesides, Torque-actuated valves for microfluidics. *Anal. Chem.* **77**, 4726–4733 (2005).
9. R. Yokokawa, T. Saika, T. Nakayama, H. Fujita, S. Konishi, On-chip syringe pumps for picoliter-scale liquid manipulation. *Lab Chip* **6**, 1062–1066 (2006).
10. B. J. Berron, A. M. May, Z. Zheng, V. Balasubramaniam, C. N. Bowman, Antigen-responsive, microfluidic valves for single use diagnostics. *Lab Chip* **12**, 708–710 (2012).

11. J. Ter Schiphorst, J. Saez, D. Diamond, F. Benito-Lopez, A. P. H. J. Schenning, Light-responsive polymers for microfluidic applications. *Lab Chip* **18**, 699–709 (2018).

12. J. K. Hamilton, M. T. Bryan, A. D. Gilbert, F. Y. Ogrin, T. O. Myers, A new class of magnetically actuated pumps and valves for microfluidic applications. *Sci. Rep.* **8**, 933 (2018).

13. L. D'Eramo, B. Chollet, M. Leman, E. Martwong, M. Li, H. Geisler, J. Dupire, M. Kerdraon, C. Vergne, F. Monti, Y. Tran, P. Tabeling, Microfluidic actuators based on temperature-responsive hydrogels. *Microsystems Nanoeng.* **4**, 17069 (2018).

14. E. Samiei, M. Tabrizian, M. Hoorfar, A review of digital microfluidics as portable platforms for lab-on a-chip applications. *Lab Chip* **16**, 2376–2396 (2016).

15. A. H. C. Ng, R. Fobel, C. Fobel, J. Lamanna, D. G. Rackus, A. Summers, C. Dixon, M. D. M. Dryden, C. Lam, M. Ho, N. S. Mufti, V. Lee, M. A. M. Asri, E. A. Sykes, M. D. Chamberlain, R. Joseph, M. Ope, H. M. Scobie, A. Knipes, P. A. Rota, N. Marano, P. M. Chege, M. Njuguna, R. Nzunza, N. Kisangau, J. Kiogora, M. Karuingi, J. W. Burton, P. Borus, E. Lam, A. R. Wheeler, A digital microfluidic system for serological immunoassays in remote settings. *Sci. Transl. Med.* **10**, eaar6076 (2018).

16. M. Boyd-Moss, S. Baratchi, M. Di Venere, K. Khoshmanesh, Self-contained microfluidic systems: A review. *Lab Chip* **16**, 3177–3192 (2016).

17. Y. Song, B. Lin, T. Tian, X. Xu, W. Wang, Q. Ruan, J. Guo, Z. Zhu, C. Yang, Recent progress in microfluidics-based biosensing. *Anal. Chem.* **91**, 388–404 (2019).

18. D. Juncker, H. Schmid, U. Drechsler, H. Wolf, M. Wolf, B. Michel, N. de Rooij, E. Delamarche, Autonomous microfluidic capillary system. *Anal. Chem.* **74**, 6139–6144 (2002).

19. A. W. Martinez, S. T. Phillips, Z. Nie, C.-M. Cheng, E. Carrilho, B. J. Wiley, G. M. Whitesides, Programmable diagnostic devices made from paper and tape. *Lab Chip* **10**, 2499–2504 (2010).

20. E. Fu, B. Lutz, P. Kauffman, P. Yager, Controlled reagent transport in disposable 2D paper networks. *Lab Chip* **10**, 918–920 (2010).

21. E. Fu, C. Downs, Progress in the development and integration of fluid flow control tools in paper microfluidics. *Lab Chip* **17**, 614–628 (2017).

22. A. Olanrewaju, M. Beaugrand, M. Yafia, D. Juncker, Capillary microfluidics in microchannels: From microfluidic networks to capillaric circuits. *Lab Chip* **18**, 2323–2347 (2018).

23. Y. Arango, Y. Temiz, O. Gökçe, E. Delamarche, Electrogates for stop-and-go control of liquid flow in microfluidics. *Appl. Phys. Lett.* **112**, 153701 (2018).

24. J. Oliver, C. Huh, S. Mason, Resistance to spreading of liquids by sharp edges. *J. Colloid Interface Sci.* **59**, 568–581 (1977).

25. W. Satoh, M. Loughran, H. Suzuki, Microfluidic transport based on direct electrowetting. *J. Appl. Phys.* **96**, 835–841 (2004).

26. P.-G. de Gennes, F. Brochard-Wyart, D. Quéré, *Capillarity and Wetting Phenomena: Drops, Bubbles, Pearls, Waves* (Springer, 2004).

27. R. Gorkin, J. Park, J. Siegrist, M. Amasia, B. S. Lee, J.-M. Park, J. Kim, H. Kim, M. Madou, Y.-K. Cho, Centrifugal microfluidics for biomedical applications. *Lab Chip* **10**, 1758–1773 (2010).

28. P. Vulto, S. Podszun, P. Meyer, C. Hermann, A. Manz, G. A. Urban, Phaseguides: A paradigm shift in microfluidic priming and emptying. *Lab Chip* **11**, 1596–1602 (2011).

29. E. Kreit, M. Dhindsa, S. Yang, M. Hagedon, K. Zhou, I. Papautsky, J. Heikenfeld, Laplace barriers for electrowetting thresholding and virtual fluid confinement. *Langmuir* **26**, 18550–18556 (2010).

30. Y. Temiz, E. Delamarche, 'Chip-olate' and dry-film resists for efficient fabrication, singulation and sealing of microfluidic chips. *J. Micromech. Microeng.* **24**, 097001 (2014).

31. W. C. Nelson, C.-J. Kim, Droplet actuation by electrowetting-on-dielectric (EWOD): A review. *J. Adhes. Sci. Technol.* **26**, 1747–1771 (2012).

32. A. Banerjee, E. Kreit, Y. Liu, J. Heikenfeld, I. Papautsky, Reconfigurable virtual electrowetting channels. *Lab Chip* **12**, 758–764 (2012).

33. Y. Temiz, E. Delamarche, Sub-nanoliter, real-time flow monitoring in microfluidic chips using a portable device and smartphone. *Sci. Rep.* **8**, 10603 (2018).

34. C. Dincer, R. Bruch, A. Kling, P. S. Dittrich, G. A. Urban, Multiplexed point-of-care testing – xPOCT. *Trends Biotechnol.* **35**, 728–742 (2017).

35. B. K. McKenna, J. G. Evans, M. C. Cheung, D. J. Ehrlich, A parallel microfluidic flow cytometer for high-content screening. *Nat. Methods* **8**, 401–403 (2011).

36. R. Safavieh, D. Juncker, Capillarics: Pre-programmed, self-powered microfluidic circuits built from capillary elements. *Lab Chip* **13**, 4180–4189 (2013).

37. J. Berthier, K. A. Brakke, E. Berthier, *Open Microfluidics* (John Wiley & Sons, Inc., Hoboken, NJ, USA, 2016).

38. G. C. Randall, P. S. Doyle, Permeation-driven flow in poly(dimethylsiloxane) microfluidic devices. *Proc. Natl. Acad. Sci. U.S.A.* **102**, 10813–10818 (2005).

39. H. Gau, S. Herminghaus, P. Lenz, R. Lipowsky, Liquid morphologies on structured surfaces: From microchannels to microchips. *Science* **283**, 46–49 (1999).

40. Y. Huang, A. J. Mason, Lab-on-CMOS integration of microfluidics and electrochemical sensors. *Lab Chip* **13**, 3929–3934 (2013).

41. Y. Song, Y. Zhang, P. E. Bernard, J. M. Reuben, N. T. Ueno, R. B. Arlinghaus, Y. Zu, L. Qin, Multiplexed volumetric bar-chart chip for point-of-care diagnostics. *Nat. Commun.* **3**, 1283 (2012).

42. O. Gökçe, S. Castonguay, Y. Temiz, T. Gervais, E. Delamarche, Self-coalescing flows in microfluidics for pulse-shaped delivery of reagents. *Nature* **574**, 228–232 (2019).

43. A. Bernard, B. Michel, E. Delamarche, Micromosaic immunoassays. *Anal. Chem.* **73**, 8–12 (2001).

Citation: Y. Arango, Y. Temiz, O. Gökçe, E. Delamarche, Electro-actuated valves and self-vented channels enable programmable flow control and monitoring in capillary-driven microfluidics. *Sci. Adv.* **6**, eaay8305 (2020).